Positronium

Physics Laboratory report

Group 28: Attilio Crognale and Javier Mariño Villadamigo

November 27, 2021

Contents

1 Introduction

The positronium is a bound state formed by an electron an its anti-particle, the positron. It is mainly formed by positrons emitted in β^+ decays when they encounter an atomic or free electron. When the energy of the positron is reduced to thermal energies, it has a high probability of being captured by an electron, forming, this way, the bound state of both.

The levels of positronium are similar to those of the hydrogen atom (they only differ by a factor of 2 in the energy spacing) and the lowest level is split into two different configurations of spin:

- *Parapositronium*: positron and electron are coupled in a singlet ($S = 0$). By selection rules, this state mainly annihilates through the emission of two antiparallel photons of 511 keV. The *parapositronium* has a lifetime of about 125 ps in vacuum.
- *Orthopositronium*: positron and electron are coupled in a triplet ($S = 1$). This state annihilates mainly through the emission of 3 photons, with respective energies such that energy and momentum conservation are satisfied. Its mean lifetime is 142 ns, about three orders of magnitude higher than that of *parapositronium*.

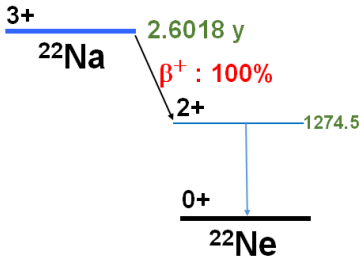

Figure 1: ^{22}Na decay scheme.

As a consequence of the difference in their lifetimes, the ratio between the emission of 3 photons and 2 photons is about $\sim 1/373$. In this experiment, the lifetimes of the two state configurations will be extracted, as well as the ratio of emission. To achieve this, it is then necessary to detect up to three photons in coincidence at the emission plane, but in order to be able to measure the lifetime of the *positronium*, its moment of creation needs to be determined.

The β^+ emitter that used in the experiment is a source of ^{22}Na, which decays through the emission of a positron to an excited state of ^{22}Ne (see Fig. 1). By detecting the photon of the de-excitation of the neon, the moment of creation of positron is determined. Detecting this 1275 keV photon requires a fourth detector, outside of the detection plane, used as the start signal for the TAC. The TAC (*Time to Amplitude Converter*) is a module used to measure the time between two signals. That way, the TAC will acquire from a START signal (in this case, the decay of Ne) to a STOP signal (in this case, the detection of 2 or 3 photons).

2 Experimental setup

In this experiment, the setup that was used consisted of several components:

- A ^{22}Na source.

- Four inorganic scintillator detectors of NaI(Tl) coupled to their respective photomultipliers.
- A FAN-IN-FAN-OUT module.
- Four constant fraction discriminators (one for each detector), that are used to get an output independent from the amplitude of the input signal.
- A TAC, to measure the lifetime of the positronium.
- A coincidence unit, to implement logic gates.
- A digitizer, to acquire the signal in a human-readable way.
- A delay unit used in the calibration of the TAC.
- A CAEN scalar module used to count directly the number of events from the coincidence unit.

The arrangement of the components detailed in the previous list is schematically displayed in Fig. 2, although is not of the highest relevance for the physics content of this work.

3 Calibration processes

In order to achieve reliable results, a calibration prior to the measurement is needed and, in particular, a calibration for each detector that provides a relation between energy and acquisition channels and a calibration for TAC that provides a relation between time delay and acquisition channels.

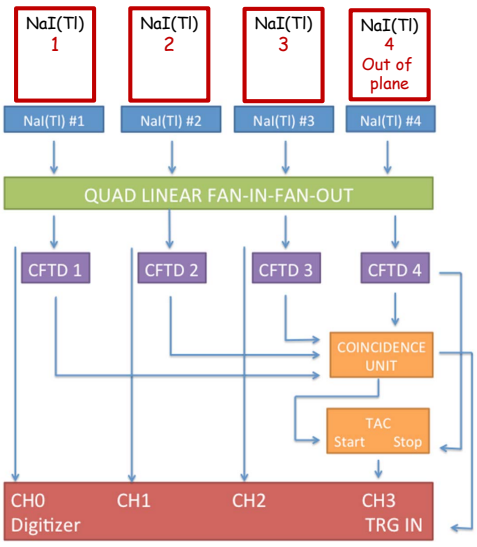

Figure 2: Electronics setup of the acquisition system.

3.1 Calibration of the detectors

For the calibration of the detectors, a standard procedure was followed: a ^{22}Na spectrum was recorded with each of the four detectors, obtaining a spectrum with the two main peaks located at certain channels. By fitting them to a gaussian curve (see Fig. 3), the mean and FWHM of each peak is obtained. Knowing that they correspond to a certain value of energy, it is then possible to extract the correspondence $E(\text{ch})$, which is shown in the last two columns of Table 1 and that will be used to obtain the corresponding energy of a channel in every detector.

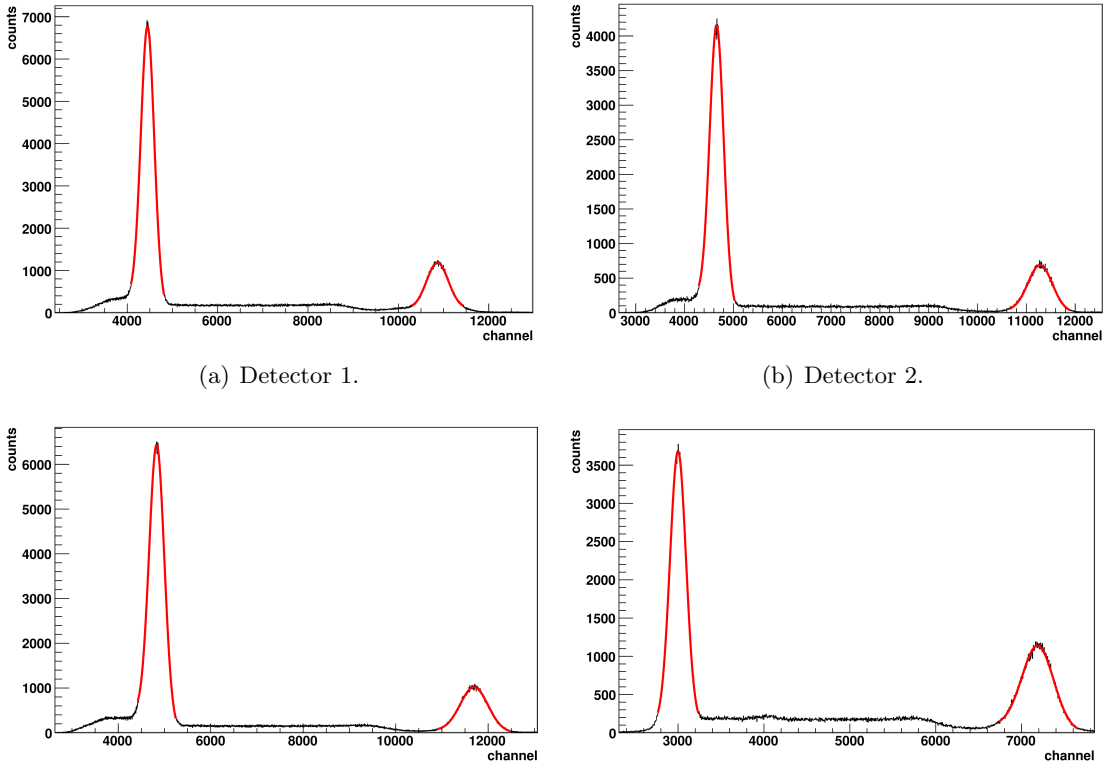

(a) Detector 1.

(b) Detector 2.

(c) Detector 3.

(d) Detector 4.

Figure 3: Peak finding and gaussian fits of the two main peaks from ^{22}Na spectra for each detector. The most relevant results of the fits (i.e. χ^2/Ndf and resolution in every peak) are shown in Table 1.

	511 keV peak		**1275 keV peak**		**Cal. E = a+b·channel**	
	χ^2**/Ndf**	**Res. (%)**	χ^2**/Ndf**	**Res. (%)**	**a**	**b**
Detector #1	1.21	7.79	1.21	5.19	-18.9(1.8)	0.11908(22)
Detector #2	1.57	7.20	1.57	5.19	-28.3(1.8)	0.11569(22)
Detector #3	1.53	7.95	1.53	6.01	-25.3(1.8)	0.11085(21)
Detector #4	1.19	7.30	1.19	6.03	-36.1(1.9)	0.18225(34)

Table 1: Results of the calibration of the detectors. The two peaks of ^{22}Na were properly fitted to a gaussian curve with good χ^2/Ndf values, obtaining better resolutions for the most energetic one. The equivalence of channel *vs* energy is shown in the last two columns, which will be used for the rest of the experiment.

3.2 TAC calibration

Using the delay unit provided among the various electronics devices, it was possible to calibrate the TAC. The PROMPT CFTD output from detector 4 was used as the START of the TAC, while the output of the coincidence unit between detector 1 and 2 was connected to the delay unit, and then used as the STOP signal for the TAC. The output of the TAC was recorded by the digitizer and acquired as a spectrum. The delay was changed manually via the delay unit, then, for each delay, a spectrum was recorded and the peak was fitted using a guassian distribution in order to find the centroid.

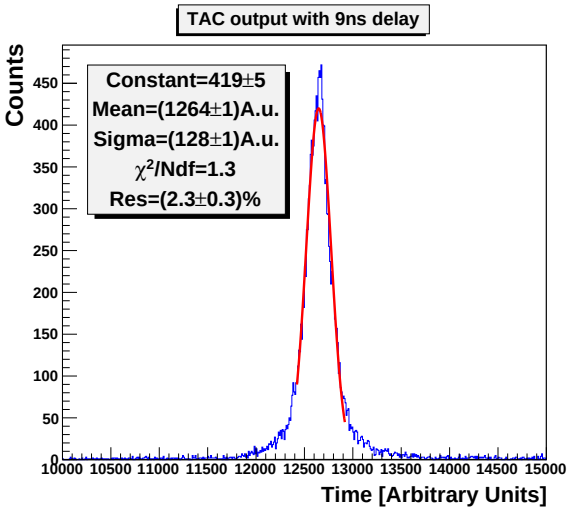

Figure 4: Example of a TAC spectrum.

By this point, a correspondence between discrete values of imposed delays and the centroids position in channels was achieved. Then, linearly fitting these points, a direct relation between TAC channels and delay is achieved, as depicted in Fig. 5.

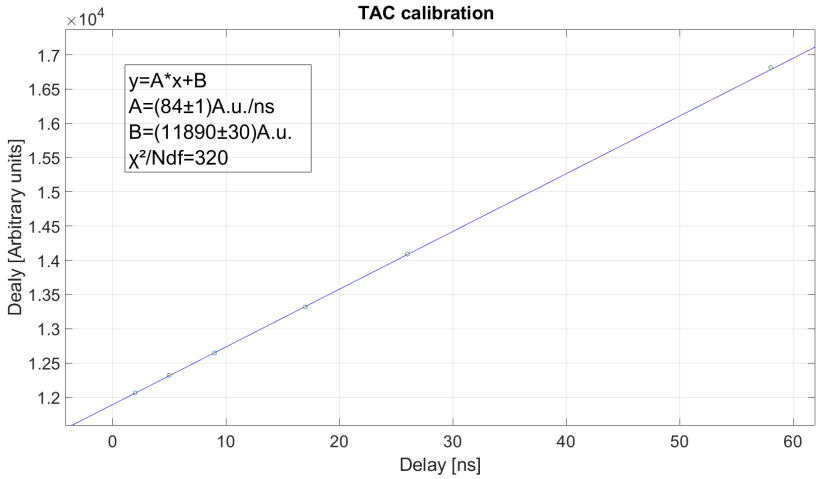

Figure 5: Linear fit for the TAC calibration.

The behavior shown in Fig. 5 is visibly linear, even though the value of χ^2/Ndf turns out to be much greater than expected. However this is most likely due to the small errors associated to each measurement. The calibration is still considered valid.

4 Measurements and results

Once the detectors and the TAC module are calibrated, it is possible to start acquiring measures with the electronics set up for the coincidence detection. The electronics configuration will be different for both setups, and the detectors should be placed colinearly (2 detectors will be used in case of 2-photon configuration) or separated by an angle of 120° (using the three in-plane detectors for the 3-photon configuration). In both cases, detector 4 (allocated vertically above the sources-detectors plane) will be set as the START signal for the TAC, as it corresponds to the decay of ^{22}Na.

4.1 Detection of coincidences

4.1.1 Two-photon configuration

In the case of two photons decay, only detectors 1, 2 and 4 were used. Detectors 1 and 2 were placed facing each other forming an angle of $\theta_{1,2} = 180°$. The signal from detector 4 was used as the START of the TAC, while the coincidence between detectors 1 and 2 was used both as the STOP of the TAC and the MASTER TRIGGER for the acquisition. Ideally, detector 4 should measure a photon of 1275 keV produced at the same time as the β^+ decay, while detectors 1 and 2 should measure one 511 keV photon each, resulting in a coincidence. The sum of the energies measured in the detectors 1 and 2 should add up to 1022 keV. However, the detectors are at a distance of about 15 cm from the source, and have about 9.5 cm diameter of aperture, therefore they subtend a certain solid angle. This angular aperture corresponds, kinematically, to a certain energy range of incoming photons around 511 keV. In this case, the photons are expected to have a certain energy distribution around 511 keV. The energy spectra for detectors 1 and 2 are shown in Fig. 6.

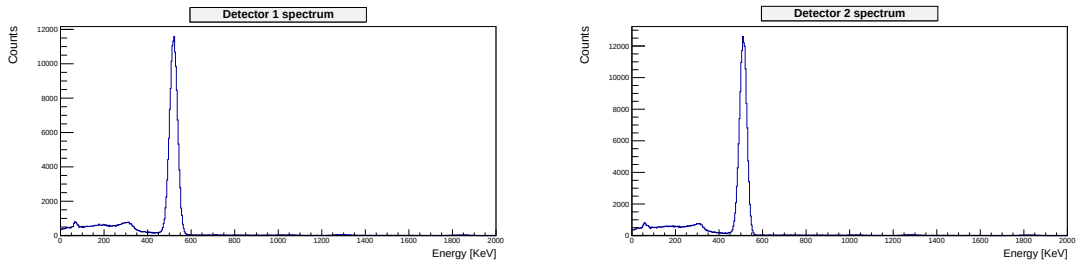

(a) Detector 1.

(b) Detector 2.

Figure 6: Spectra recorded from detector 1 (left) and 2 (right) for the measurement of 2-photon coincidences. In both spectra only the 511 keV peak is present, as expected.

By comparing the Fig. 6 and the Fig. 3, it is easy to see that taking the coincidence between detectors 1 and 2 cuts off most of the undesired events. However, the spectra above are to be filtered more precisely in order to make sure only the correct 2 photon decays are taken into account. This issue will be discussed further in the report.

4.1.2 Three-photon configuration

As stated in the introduction, the *orthopositronium* (which is the level state that decays primarily through the emission of three photons) has a lifetime three orders of magnitude higher than *parapositronium*. Therefore, the event recording time should be considerably longer. Indeed, the detectors were left on, acquiring data overnight from the second day of laboratory to the third and last.

Similarly to the 2-photon case, the output of detector 4 was used as the START of TAC, while the coincidence between detectors 1, 2 and 3 was used both as the STOP of the TAC and the MASTER TRIGGER for the acquisition. In order to be able to distinguish photons coming from the decay of positronium, the 3 detectors were set at a relative angle of 120°. In this way, these incoming photons would have an equal distribution of the 1022 keV initial energy (i.e. about 341 keV each). Also in this case, the solid angle covered by the detectors should be taken into account, but the energy distribution is expected to be much wider, because the decay has more kinematical configurations in the phase space.

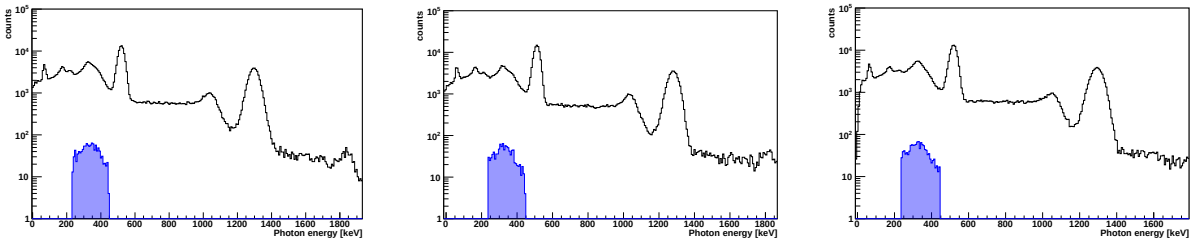

(a) Detector 1. (b) Detector 2. (c) Detector 3.

Figure 7: Events recorded from each detector (in black) and the events selected as possible 3-photon events (in shaded blue).

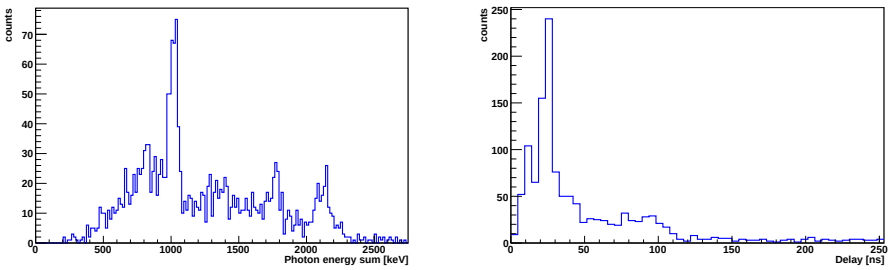

(a) Sum spectrum. (b) TAC spectrum.

Figure 8: Sum spectrum (left) and TAC spectrum (right) recorded from the 3-photon events selected in Fig. 7. It can be clearly identified a peak around 1022 keV in the sum spectrum, as expected.

The procedure of events selection that was followed can now be detailed more in-depth:

1. From each detector, those events that corresponded to photons with an energy in the range

above detailed, were selected. Additionally, the elapsed time since the capture of the 1275 keV photon in the fourth detector should remain smaller than 600 ns. As stated previously, the lifetime of *orthopositronium* is about 142 ns, so this is to ensure that the majority of residual photons coming from other interactions (such as Compton) are suppressed as much as possible. In Fig. 7 this step is depicted.

2. If the previous condition is satisfied from any of the 3 in-plane detectors, having recorded, the rest of them, an event with the same timestamp, then the sum of the three energies deposited in the detectors is stored in the histogram depicted in Fig. 8(a).

3. Finally, also the TAC spectrum is filled with the corresponding event from the sum spectrum, as shown in Fig. 8(b).

Although it is clear that most of the events energy sum up to 1022 keV (see Fig. 8(a)), there are also two accumulation zones around 1800 keV and 2150 keV. The latter could be explained from the fact that once recorded a ∼341 keV event, the other photons could actually proceed from two different *parapositronium* decays (since they should be colinear and the detectors have an angular separation of 120°), given the fact that they are about 373 times more frequent. As to the other peak, however, a possible explanation could come from the situation where two ∼341 keV photons are recorded from the *orthopositronium* decay, but in the third detector a ∼1275 keV photon is recorded from ^{22}Na decay, giving place to a 2150 keV peak.

4.2 Time distribution

4.2.1 Two-photon configuration

The time distribution of the events can be studied from the TAC signal, which should be proportional to the decay time of the *parapositronium*. The value of the mean lifetime is expected to be of the order of magnitude of the lifetime in vacuum, where $\tau = 125$ ps.

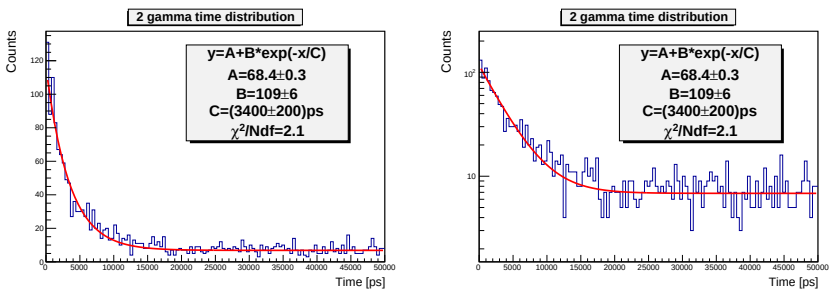

(a) Simple exponential fit. (b) Simple exponential fit (log scale).

Figure 9: Time distributions for the 2-photon configuration fitted with an exponential function presented (a) linearly scaled and (b) logarithmically scaled.

The time distribution follows an exponential behavior, where only one decay time seems to be present, as a priori expected. However, the decay time obtained by the exponential fit is

one order of magnitude greater than the one expected. This issue is justifiable by taking into account that the acquisition system has a finite resolution of about 2.3 %, as shown in Fig. 4. In terms of time units, the resolution is of the order of $1 - 10$ ns. Given these limitations from the apparatus, it could be difficult to measure a lifetime of the order of 10^{-1} ns.

In order to take into account the resolution of the system, the fitting function for Fig. 9 was modified by adding a gaussian distribution on top of the exponential decay, obtaining the following expression:

$$y = A + N_1 \exp\{-(t - t^*)^2/2\sigma^2\} + N_2 \exp(-t/\tau). \tag{1}$$

It must be stressed that this procedure is not necessarily formal but it is to be considered as an attempt to include all the contributions to the analysis. This operation is justifiable by acknowledging the fact that the resolution of the system will cause the events to spread more widely in the TAC spectrum, resulting in a longer lifetime value. Some parameters of the gaussian had to be fixed in order to have a converging fit, in particular $N_1 = 140$ and $t^* = 0$. The modified fit is presented in Fig. 10.

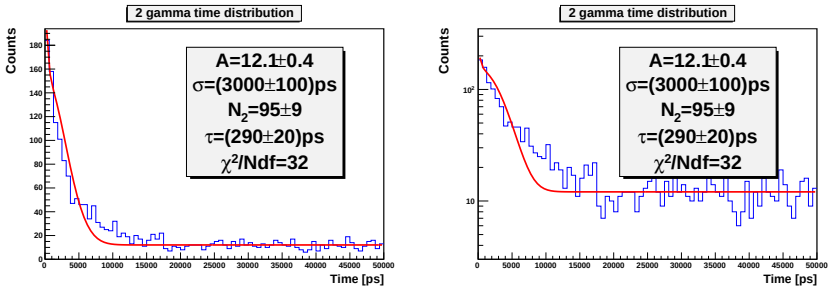

(a) Time distribution fitted with Eq. 1. (b) Time distribution fitted with Eq. 1 (log scale).

Figure 10: Time distributions for the 2-photon configuration fitted to Eq. 1 presented (a) linearly scaled and (b) logarithmically scaled.

The fit shown in Fig. 10 is visibly worse than the one in Fig. 9, and also the value of the χ^2/Ndf increases significantly. However, by introducing the gaussian distribution it was possible to retrieve a better value for the decay time of *parapositronium*. In fact, as shown in Fig. 10, the new value for the lifetime is $\tau = 290(20)$ ps, which is, at least, the same order of magnitude of the expected result $\tau_{expected} = 125$ ps.

4.2.2 Three-photon configuration

The time distribution of the events in the case of the emission of three photons is a little bit more complicated because of the precision that is required to filter the data as much as possible without eliminating the few 3-photon events. Nonetheless, by fitting the time distribution of the events to the sum of two exponential decays, i.e.:

$$N = \exp\{-t/\tau_1 + a\} + \exp\{-t/\tau_2 + b\}, \tag{2}$$

it is possible to get a reasonably good approach to the two lifetimes components.

In Fig. 11, it can be seen that a reasonably good fit was obtained for the time distribution of the events involving 3-photon coincidences, with two lifetime components of $\tau_1 = 45.0(2.8)$ ns and $\tau_2 = 2.40(56)$ ns, respectively. These results differ significantly from those obtained for mesoporous silicon ($\tau_1 = 140(7)$ ns and $\tau_1 = 25.0(3)$ ns) and for vacuum ($\tau = 142$ ns).

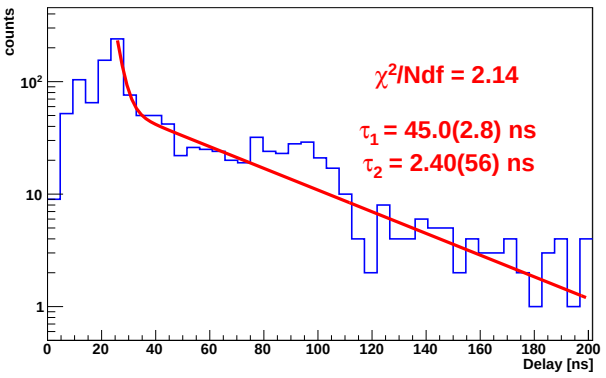

Figure 11: Fit of Eq. 2 to the TAC spectrum shown in Fig. 8(b), corresponding to 3-photon events.

The discrepancy with the value for vacuum could be a priori explained from the point of view of available electrons, more numerous in air, and therefore the positronium would be created shortly after the decay and the measured lifetime would be smaller. However, it could also be due to the fact that the *parapositronium* events so far considered are unfiltered, given the fact that it would be possible for one photon of 511 keV to enter the detector with an angular aperture such that it could overlap with the energy range of 341 keV photons.

4.3 The sum spectra and the ratio between the two configurations

In Fig. 12, the energies of the hypothetical coincidence photons are represented summed over. As can be deduced from the number of entries and the shape of each histogram, it is clear that 2-photon events have a more uniform measurement of the distribution of energies, while the 3-photon events have a wider distribution, mainly due to the reasons mentioned in section 4.2.2.

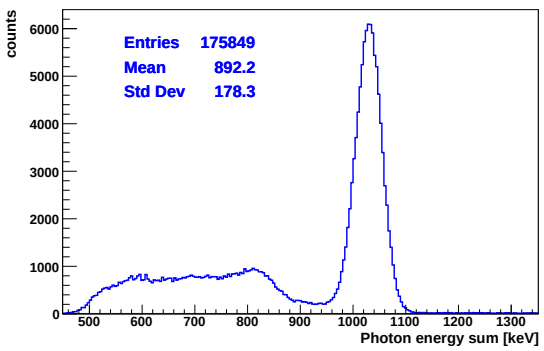

(a) Sum spectrum from 2-photon configuration.

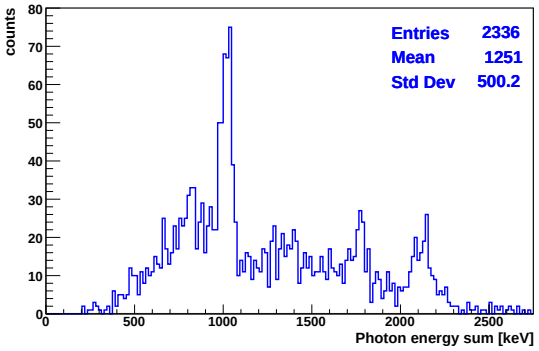

(b) Sum spectrum from 3-photon configuration.

Figure 12: Sum spectra of energies for two-photon events (left) and three-photon events (right). Note that both of them have the main accumulation point around ∼1022 keV, as expected.

To extract now the ratio between the emission of 2 and 3 photons, it is necessary to count the events that truly belong to the coincidence of two ∼511 keV photons and three ∼341 keV photons, respectively. To do that, the approach followed in this report was to fit the main accumulation point around 1022 keV in the spectra showed in Fig. 12 to a gaussian curve plus a first degree polynomial and, then, compute the integral of such fit in an interval given by 3σ. Following this method, the amount of events N with mean μ and standard deviation σ should be accounted for in the integral with a 99.6 % probability:

$$N = \int_{\mu-3\sigma}^{\mu+3\sigma} \left[\frac{1}{\sigma\sqrt{2\pi}} \exp\left\{(x-\mu)^2/2\sigma^2\right\} + (a + b \cdot x) \right] dx. \tag{3}$$

These results are shown in Fig. 13, where the integral is depicted as the shaded red area under the red curve. As it can be seen, the fit for 3-photon configuration is slightly better with a value χ^2/Ndf closer to 1.

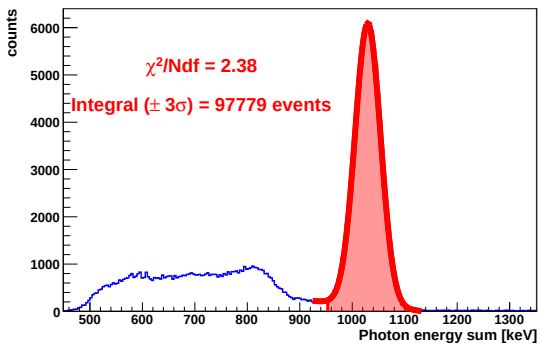

(a) Fitted sum spectrum for two-photon configuration.

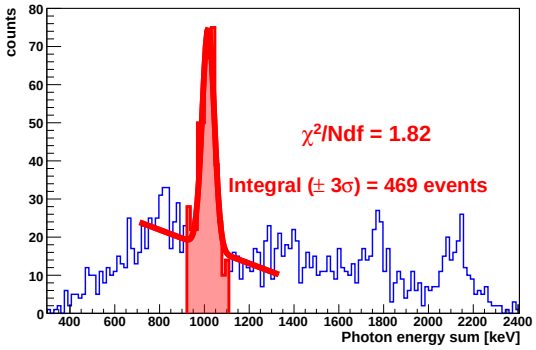

(b) Fitted sum spectrum for three-photon configuration.

Figure 13: Sum spectra for two- (left) and three- (right) photon configuration, fitted to the Eq. 3.

On top of these results, it is also important to take into account the dead time of the acquisition, in order to make proper corrections to the number of events. The dead time was extracted from a separate sample of measurements, where the number of counts displayed by the acquisition system was compared the number of counts given by a scalar counting module connected to the coincidence unit. In the case of 2-photon decays the counting rate was of the order of 5 kHz and the dead time was measured to be 4 %. The number of events from 2 gamma decays is therefore increased by the same factor. In the case of 3-photon decays the counting rate was of the order of 5 Hz, and the dead time was measured to be practically zero.

Now, it is necessary to normalize the number of events acquired for each experience by taking into account the acquisition time. As it was commented before, the 3-photon experience was carried out overnight, for a total amount of time of 20 hours, 22 minutes and 17 seconds, while the two-photon experience can be carried out much faster, in a total time of 1 hour and 1 minute. Expressing all in seconds:

$$t_{2\gamma} = 3660 \text{ s}, \qquad t_{3\gamma} = 73337 \text{ s}.$$

Therefore, taking into account that $N_{2\gamma} = 97779$ and $N_{3\gamma} = 469$, then the ratio yields:

$$\boxed{R = n_{3\gamma}/n_{2\gamma} \approx 2.41(13) \cdot 10^{-4}},$$

where the error for the number of events was taken as $\sigma_N = \sqrt{N}$. This result differs greatly from the expected value of 1/373.

However, an important comment is necessary. As explained in section 4.2.2, the energy spread of the sum of 3-photon configuration is higher than in 2-photon configuration due to the infrequency with which 3 photons are emitted. Therefore, by "assuming" that one of the 341 keV is being captured, while the other detectors are having contributions from other decays (remember that TAC has a time resolution of 2 ns and the lifetime of *parapositronium* is 125 ps), it is possible to count all the spectrum shown in Fig. 13(b) as actual 3-photon events.

Doing that, one gets $N_{3\gamma} = 1970 \pm 40$ events instead of 469, and repeating the procedure the total ratio yields a result of:

$$\boxed{R \approx 1.004(23) \cdot 10^{-3} \approx 1/996},$$

which is still about 3 times smaller than the actual ratio, but the same order of magnitude.

5 Conclusions

In both decay configurations it was verified that the time distribution of the events follows and exponential pattern.

In the case of the 2-photon configuration, only one decay time was observed. Because of the resolution of the system, it was not possible to obtain a satisfying estimate of the decay time via simple exponential fit. However implementing a more complex function, Eq. 1, that would take into account the presence of a finite resolution, resulted in better value for the decay time, namely $\tau = 290(20)$ ps. This estimate is almost three times bigger than the expected value of 125 ps, but is the best one achieved given the limitations of the apparatus.

In the case of the 3-photon decay configuration, it was possible to confirm that, as expected, *orthopositronium* presents 2 different decay times if produced inside a material. In particular, it was possible to distinguish between a short time component, with lifetime $\tau_2 = 2.40(56)$ ns, and a long time component, with lifetime $\tau_1 = 45.0(2.8)$ ns.

The counting rate in 2-photon configuration was estimated to be about 5000 times higher than that in 3-photon configuration. Expanding the event selection in the 3-photon sum spectrum based on energy dispersion arguments, a closer to the theoretical value of 1/373 was achieved, obtaining a final ratio of about 1/996.